



CORROSION INHIBITION AND ADSORPTION BEHAVIOUR OF (2E)-2-(3-HYDROXY-2-METHOXYBENZYLIDENE) HYDRAZINECARBOTHIAMIDE ON MILD STEEL IN 1 M HCL

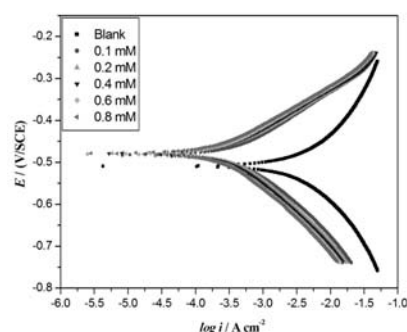
Preethi KUMARI P,^a Prakash SHETTY,^{b,*} Suma A RAO,^a Dhanya SUNIL^A

^a Department of Chemistry, Manipal Institute of Technology, Manipal University, Manipal, 576104, India

^b Department of Printing and Media Engineering, Manipal Institute of Technology, Manipal University, Manipal, 576104, India

Received February 24, 2014

Corrosion behaviour of mild steel in 1 M hydrochloric acid solution containing various concentrations of (2E)-2-(3-hydroxy-2-methoxybenzylidene) hydrazinecarbothiamide (HMBHC) was studied by Tafel polarization technique and electrochemical impedance spectroscopy technique at different temperatures. The inhibition efficiency of HMBHC increased with the increase in its concentration and in temperature. Polarization study showed that the HMBHC acted as a mixed type inhibitor and its adsorption on mild steel surface was found to follow Langmuir's adsorption isotherm. The formation of protective film was confirmed by scanning electron microscopy study.



INTRODUCTION

Mild steel is one of the most widely used engineering materials with many industrial applications. This alloy corrodes under many circumstances, particularly in chemical process industries, acid pickling, oil refinery, acidization of oil wells, acid descaling etc., and hence its corrosion study has received considerable attention by many researchers.¹ The use of organic compounds is one of the most effective and yet reasonably inexpensive methods to inhibit the corrosive attack on metals and alloys. Literature survey showed that organic compounds containing hetero atoms (such as nitrogen, sulphur, and oxygen), unsaturated bonds (such as double or triple bonds) and aromatic or heterocyclic rings functioned as effective corrosion inhibitors for mild steel and many other metals and alloys in acid media.² Hydrazides and their derivatives have continued to be subject of

extensive investigation in chemistry and biology owing to their broad spectrum of anti-tumor, antimalarial³ and many other applications including corrosion inhibition of metals. Several acid hydrazide derivatives, aromatic hydrazide derivatives, thiosemicarbazide derivatives have shown exceptional ability to inhibit corrosion of mild steel in acidic solutions.^{4,5}

The aim of the present work is to introduce a novel aromatic hydrazide derivative (2E)-2-(3-hydroxy-2-methoxybenzylidene) hydrazinecarbothiamide (HMBHC) as a corrosion inhibitor for mild steel in 1 M HCl medium using Tafel polarization and EIS methods, and to study the effect of temperatures and inhibitor concentrations on corrosion inhibition efficiency. Further the study also focuses on the inhibition mechanism by studying the adsorption isotherms, activation and thermodynamic parameters.

* Corresponding author: prakash.shetty@manipal.edu, tel: +91820-2925661, fax: +91820-2571071

EXPERIMENTAL

Synthesis of HMBHC

(2*E*)-2-(3-hydroxy-2-methoxybenzylidene) hydrazinecarbothiamide (HMBHC) was synthesized as per the reported literature.³ Fig. 1 represents the chemical structure of the inhibitor molecule. An equimolar mixture of ethanolic solution of vaniline (0.01 mol) and thiosemicarbazide (0.01 mol) was refluxed on a hot water bath for about 2 h. The product obtained was purified by recrystallization and characterized by IR spectroscopy (Schinadzu FTIR 8400S Spectrophotometer) and mass spectroscopy techniques (Agilent Technologies 1200 series).

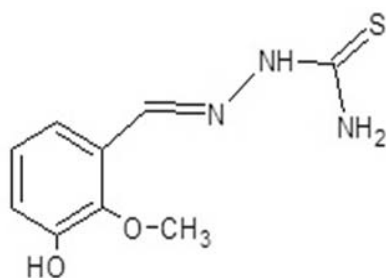


Fig. 1 – Chemical structure of HMBHC molecule.

Medium

The standard solution of 1 M HCl was prepared using AR grade hydrochloric acid and double distilled water.

Preparation of working electrode

The composition of mild steel specimen used in this corrosion study is (% wt) C (0.159), Si (0.157), Mn (0.496), P (0.060), S (0.062), Cr (0.047), Ni (0.06), Mo (0.029), Al (0.0043), Cu (0.116) and balance was iron. The working specimens were prepared in the form of a cylindrical rod embedded in epoxy resin, having one end of the rod with an open surface area of 0.95 cm². Polishing of the exposed surface was done using emery papers of different grades (400-1000). Further the polishing was done with disk polisher using levigated alumina to obtained mirror finish. The polished specimen was washed with double distilled water, rinsed with acetone and dried before immersing in to the corrosive medium.

Electrochemical measurements

Electrochemical measurements such as Tafel polarization technique and electrochemical impedance spectroscopy techniques were carried out using an electrochemical work station (CH Instrument USA Model 604D series with beta software). The electrochemical cell consisted of a conventional three-electrode Pyrex glass cell with platinum electrode as counter electrode, saturated calomel electrode (SCE) as reference electrode, and mild steel as working electrode.

Freshly polished mild steel specimen with surface area of 0.95 cm² was exposed to 1 M HCl medium at temperatures of 30 to 60 °C without, and with 0.1, 0.2, 0.4, 0.6 and 0.8 mM inhibitor concentrations in the acid solution. The steady state open circuit potential (OCP) with respect to SCE was noted at the end of 30 minutes. Impedance experiments were carried out in the frequency range 100 kHz to 0.01 Hz, at the open circuit potential by applying small amplitude ac signal of 10 mV. Nyquist plots were used to extract different

parameters like solution resistance (R_s), charge transfer resistance (R_{ct}) and the double layer capacitance (C_{dl}). The polarisation studies were made from -250 mV cathodically to +250 mV anodically versus respective OCP with a scan rate of 1 mV s⁻¹ and the corresponding corrosion current recorded.

Scanning electron microscopy (SEM)

Surface morphology of the mild steel specimen immersed in 1 M HCl in the absence and presence of optimal concentration of HMBHC was recorded by using Scanning electron microscopy EVO 18-5-57 model.

RESULTS AND DISCUSSION

Characterization of HMBHC

(2*E*)-2-(3-hydroxy-2-methoxybenzylidene) hydrazinecarbothiamide (95%) was obtained as crystalline white solid; m.p. 216-218 °C; Anal. Calcd. for C₉H₁₁N₃O₂S: C, 49; H, 5.6; N, 15.6. Found: C, 48.91; H, 5.54; N, 15.5. IR [KBr, cm⁻¹]: 1596 (C=N str.), 1296 (C=S str.), 1580 (Ar. C=C str.), 2823, 3031 (CH str.), 3147 (NH str.), 3433, 3278 (NH₂ str.), 3525(OH); m/z: 225 (M⁺).

Tafel polarization measurements

The results of Tafel polarization measurements for the corrosion of mild steel in 1 M HCl in the presence and absence of HMBHC are recorded in Table 1. The Tafel plots obtained for the specimen at different concentrations of HMBHC at 40 °C in 1 M HCl are shown in Fig. 2.

The corrosion rate (CR) is calculated using Eq. 1.

$$CR \text{ (mmpy)} = \frac{3270 \times M \times i_{corr}}{\rho \times Z} \quad (1)$$

Where the constant, 3270 represents the unit of corrosion rate, i_{corr} = corrosion current density in A cm⁻², ρ = density of the corroding material (7.74 g cm⁻³), M = Atomic mass of the metal (55.85), and Z = Number of electrons transferred per metal atom ($Z=2$).⁶

The surface coverage (θ) on the metal surface and the percentage inhibition efficiency (% IE) are calculated using Eq. (2) and (3) respectively.⁷

$$\theta = \frac{i_{corr} - i_{corr(inh)}}{i_{corr}} \quad (2)$$

Where i_{corr} and $i_{corr(inh)}$ represent the corrosion current densities in the presence of uninhibited and inhibited solution respectively.

$$\% IE = \theta \times 100 \quad (3)$$

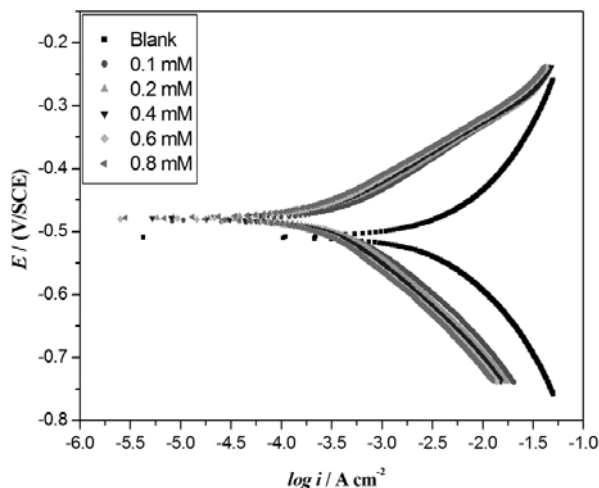


Fig. 2 – Tafel polarization curves for the mild steel specimen in 1 M HCl with various concentrations of HMBHC at 40 °C.

Table 1

Tafel polarization parameters for the corrosion studies on mild steel in 1 M HCl containing different concentrations of HMBHC

Temp (°C)	Conc. of inhibitor (mM)	E_{corr} (mV)	$-b_c$ (mVdec ⁻¹)	b_a (mV dec ⁻¹)	i_{corr} (mA cm ⁻²)	IE (%)
30	0	-507	73.14	83.05	1.894	-
	0.1	-486	81.75	105.02	0.292	84.5
	0.2	-478	80.60	103.02	0.219	88.4
	0.4	-479	77.32	105.73	0.181	90.4
	0.6	-479	79.75	103.26	0.157	91.5
	0.8	-475	80.75	106.59	0.133	92.9
40	0	-505	68.71	70.91	3.352	-
	0.1	-489	77.41	91.65	0.447	86.7
	0.2	-487	74.28	101.42	0.386	88.4
	0.4	-488	75.47	104.04	0.315	90.6
	0.6	-487	77.99	105.92	0.280	91.6
	0.8	-486	80.41	109.72	0.238	92.9
50	0	-504	61.32	77.77	5.861	-
	0.1	-504	74.69	87.94	0.750	87.1
	0.2	-495	71.10	87.10	0.693	88.3
	0.4	-499	74.16	70.85	0.547	90.7
	0.6	-504	74.06	79.87	0.438	92.5
	0.8	-508	74.80	91.16	0.380	93.6
60	0	-504	64.28	72.48	11.35	-
	0.1	-500	71.07	98.14	1.287	88.6
	0.2	-501	72.07	98.33	1.246	89.0
	0.4	-503	72.38	99.05	1.041	90.8
	0.6	-501	75.02	98.58	0.833	92.6
	0.8	-502	74.57	109.08	0.691	93.9

It is evident from the Table 1 that the corrosion current density (i_{corr}) and corrosion rate (CR) decreases considerably with increase in HMBHC concentration, while percentage inhibition efficiency (% IE) increases with increase in HMBHC concentrations as well as with increase in temperatures. The increase in % IE with increase in inhibitor concentrations is due to the blocking effect of the metal surface by both adsorption and film formation. It is also observed that there is no remarkable shift in E_{corr} either positive or negative region on the addition of HMBHC with respect to the uninhibited one. It is reported⁸ that if the shift in corrosion potential in presence of inhibitor exceeds ± 85 mV with respect to corrosion potential of the uninhibited solution, the inhibitor functions as either anodic or cathodic type. In the present case the maximum displacement in E_{corr} is well within +20 mV, and it indicates that HMBHC acts as mixed type inhibitor. Further it is observed from Table 1 that there is no appreciable change in Tafel slopes (anodic slope or cathodic slope) with increase in inhibitor concentration, which indicates that the mechanism of anodic and cathodic reaction does not alter with increase in inhibitor concentration.⁹

The addition of HMBHC brings down the corrosion rate to the minimal level, and further the inhibition efficiency increases with increase in temperature. This may be due to the fact that physisorption favours at lower temperature, whereas chemisorption at higher temperature.¹⁰ At higher temperature the inhibition efficiency increases due to increase in surface coverage (θ). The high inhibition efficiency of HMBHC is mainly due to its bonding interaction with the

metal surface. The strong bonding is generally attributed to higher electron densities at active functional groups, imine group and π electrons present in the adsorbate molecules.¹¹ These results facilitate the evaluation of kinetic and thermodynamic parameters for the inhibition and interpretation of the mode of adsorption on the metal surface by the inhibitor.

Arrhenius equation is used to calculate the activation energy (E_a) for the corrosion process in the presence and absence of HMBHC.¹²

$$\ln(CR) = B - \frac{E_a}{RT} \quad (4)$$

Where B is the Arrhenius pre-exponential constant, and R is the universal gas constant. The slope ($-E_a/R$) obtained from the plot of $\ln(CR)$ against $1/T$ is used to calculate the activation energy for the corrosion process. Arrhenius plot ($\ln CR$ vs $1/T$) for the corrosion of mild steel in 1M HCl is shown in Fig. 3. The enthalpy of activation (ΔH^\ddagger) and entropy of activation (ΔS^\ddagger) for the metal dissolution process are determined using the transition state equation (5).¹²

$$CR = \frac{RT}{Nh} \exp\left(\frac{\Delta S^\ddagger}{R}\right) \exp\left(\frac{-\Delta H^\ddagger}{RT}\right) \quad (5)$$

Where h is Plank's constant and N is Avagadro's number. Fig. 4 shows the plot of $\ln(CR/T)$ vs $1/T$, gives a straight line with slope = $-\Delta H^\ddagger/T$ and intercept = $\ln(R/Nh) + \Delta S^\ddagger/R$. The activation parameters obtained are recorded in Table 2.

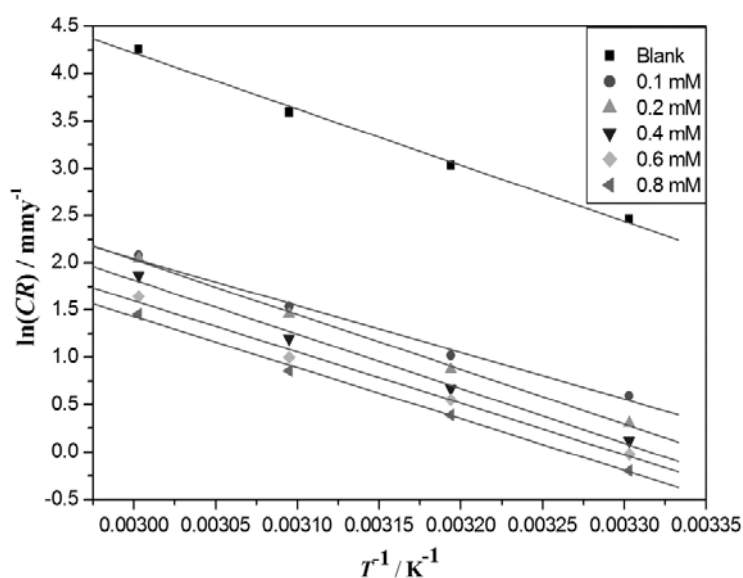


Fig. 3 – Arrhenius plots of $\ln(CR)$ vs. $1/T$ for mild steel in 1 M HCl with different concentrations of HMBHC.

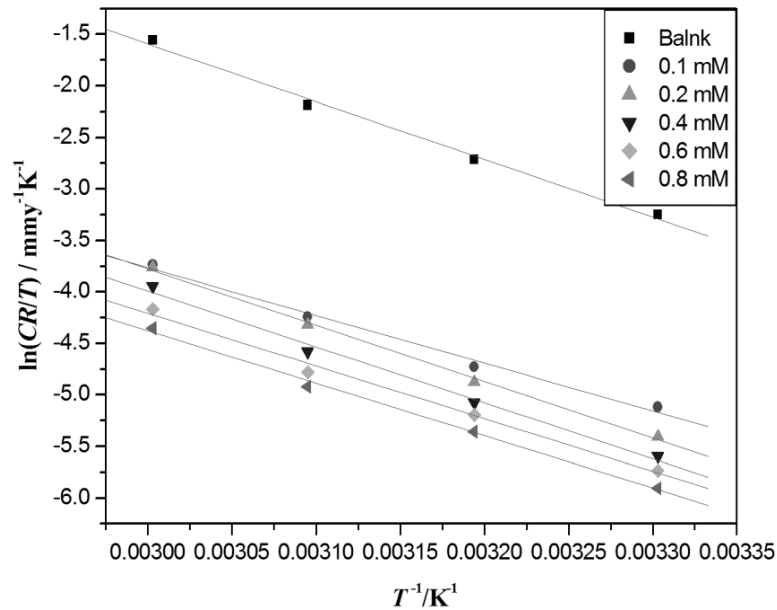


Fig. 4 – Plot of $\ln(CR)/T$ versus $1/T$ for mild steel specimen in 1 M HCl containing various concentrations of HMBHC.

Table 2

Activation parameters for the corrosion of mild steel in 1 M HCl containing different concentrations of HMBHC

Conc. of inhibitor (mM)	E_a (kJmol ⁻¹)	ΔH^\ddagger (kJmol ⁻¹)	ΔS^\ddagger (Jmol ⁻¹ K ⁻¹)
0	49.22	46.83	-71.00
0.1	41.15	38.51	-113.29
0.2	48.19	45.55	-92.26
0.4	47.78	45.14	-95.27
0.6	45.15	42.51	-104.95
0.8	44.97	42.33	-106.89

The decrease in energy of activation (E_a) with increase in inhibitor concentrations indicates that adsorption of inhibitor takes place through chemisorption. This is due to the gradual adsorption of inhibitor molecules on the mild steel with a resultant closer approach to equilibrium during the experiment at higher temperatures.¹³ The negative value of ΔS^\ddagger signifies that an increase in disordering takes place on going from reactant to the activated complex, and positive value of ΔH^\ddagger indicate the endothermic nature of steel dissolution process.¹⁴

Adsorption isotherm

Basic information on the interaction between the inhibitor and the metal surface can be provided by the adsorption isotherm, which helps to

understand the mechanism of corrosion inhibition. The adsorbed inhibitor forms a protective film at the metal/corrosive interface, which acts as barrier between the metal surface and corrosive medium.

The values of θ at different concentrations of inhibitor have been used to explain the various isotherms to fit the adsorption process. In the temperature range studied the best correlation between the experimental results and the isotherm function follows Langmuir's adsorption isotherm, which is given by the expression (7).¹⁵

$$\frac{C_{inh}}{\theta} = \frac{1}{K} + C_{inh} \quad (7)$$

Where K value represents the equilibrium constant for metal- inhibitor interaction, C_{inh} is the inhibitor concentration, and θ is the degree of surface coverage.

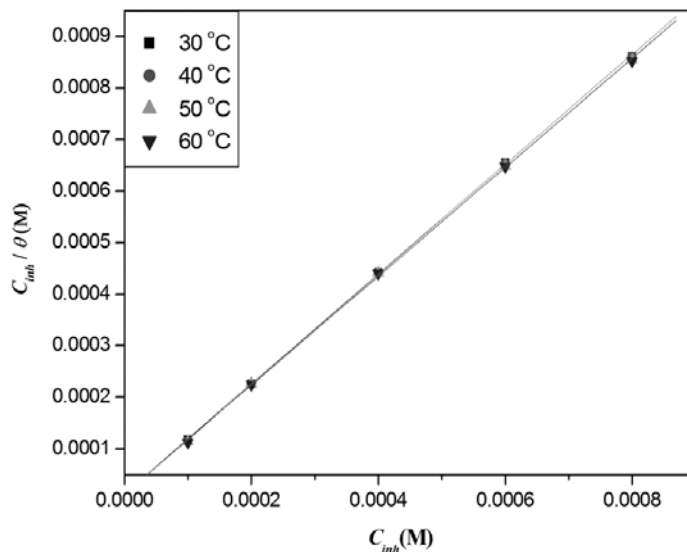


Fig. 5 – Langmuir's adsorption isotherm of HMBHC for mild steel in 1 M HCl at 40 °C.

The plot of C_{inh}/θ versus C_{inh} gives a straight line with intercept $1/K$ as shown in Fig. 5. The values of standard free energy of adsorption are related to K by the relation (8).¹⁶ The calculated values of ΔG_{ads}^0 , are tabulated in Table 3.

$$K = \frac{1}{55.5} \exp\left(\frac{-\Delta G_{ads}^0}{RT}\right) \quad (8)$$

Where R is the universal gas constant, T is the absolute temperature, and 55.5 is the concentration of water in solution in mol dm^{-3} . The isotherm that best fits the experimental data is chosen using the correlation coefficient. The correlation coefficient values are close to unity (Table 3) and the slight deviation of slopes of straight lines from unity

indicates that the adsorption of HMBHC obeys Langmuir's adsorption isotherm.¹¹ The negative values of ΔG_{ads}^0 are typical of strong spontaneous adsorption for the studied inhibitor compound, which also reflect high inhibition values.¹⁷ Generally, the standard free energy values of the order -20 kJ mol^{-1} or less negative are associated with physisorption, while -40 kJ mol^{-1} or more negative corresponds to chemisorption.¹⁸ It can be seen from Table 3 the ΔG_{ads}^0 value corresponding to lower temperature (30 °C) indicates the physisorption, whereas the values corresponds to higher temperature (60 °C) indicating chemisorption.¹⁹ Hence the inhibitor shows mixed adsorption behaviour. A plot of ΔG_{ads}^0 versus T obtained with straight line is shown in Fig. 6.

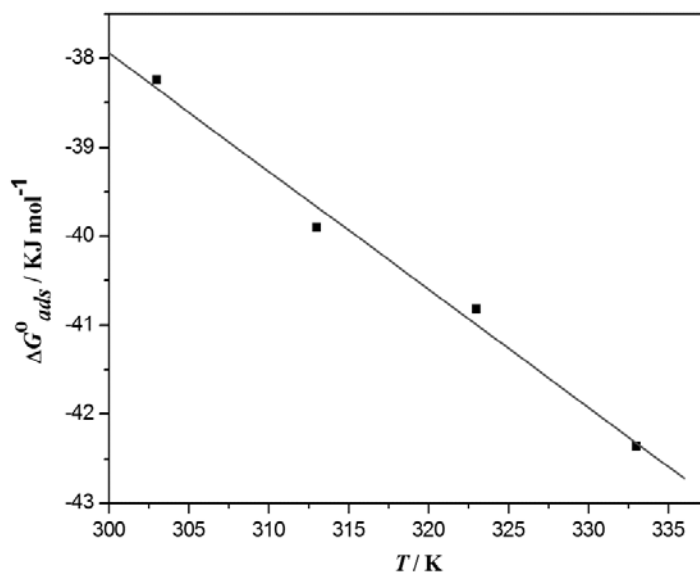


Fig. 6 – Plot of ΔG_{ads}^0 versus temperature for the adsorption of HMBHC on Mild steel in 1 M HCl.

Table 3

Thermodynamic parameters for the adsorption of HMBHC on mild steel surface in 1 M HCl at different temperatures

Temperature (°C)	ΔG_{ads}° (kJ mol ⁻¹)	Correlation coefficient Slope	ΔH_{ads}° (kJ mol ⁻¹)	ΔS_{ads}° (Jmol ⁻¹ K ⁻¹)
30	-38.24	0.999	1.063	1.9004
40	-39.90	0.999	1.065	
50	-40.82	0.999	1.055	
60	-42.36	0.999	1.054	

The standard enthalpy of adsorption (ΔH_{ads}°) and the standard entropy of adsorption (ΔS_{ads}°) are computed from the slope and intercept of the straight line respectively according to the thermodynamic equation (9) and, the results are recorded in Table 3.

$$\Delta G_{ads}^{\circ} = \Delta H_{ads}^{\circ} - T \Delta S_{ads}^{\circ} \quad (9)$$

The negative value (Table 3) of ΔS_{ads}° indicates that an ordering takes place when the inhibitor gets adsorbed on the metal surface. The positive value of ΔH_{ads}° indicates that the adsorption of inhibitor molecules is an endothermic process. Generally an exothermic adsorption process signifies either physisorption or chemisorption while the endothermic process is attributed to chemisorption.²⁰ In the present study, the calculated value of ΔH_{ads}° is greater

than zero (1.9004 kJ mol⁻¹), which indicates the chemisorption of HMBHC on the metal surface.

Electrochemical impedance spectroscopy

The Nyquist plots for the corrosion of mild steel in the absence and in the presence of various concentrations of the HMBHC are shown in Fig. 7.

Impedance plots are obtained with depressed semicircles in the presence of inhibitor and the diameter of the semicircles increases with increase in inhibitor concentrations. This indicates that the charge transfer process is mainly controlling the corrosion of mild steel. The depressed capacitive behaviour can be attributed to the contribution from roughness of the surface, active sites distribution or inhibitor adsorption.²¹

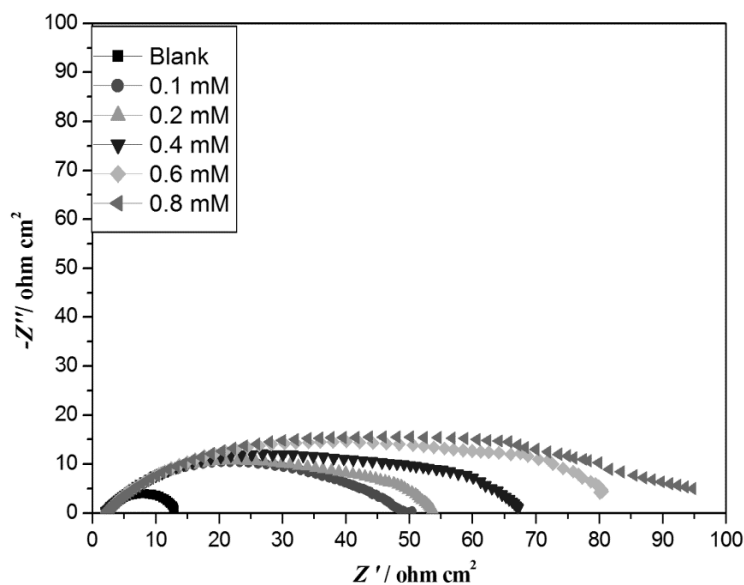


Fig. 7 – Nyquist plots for mild steel specimen in 1 M HCl acid containing different concentrations of HMBHC at 40 °C.

The impedance parameters are analysed by fitting suitable equivalent circuit to the Nyquist plots using ZSimpWin software version 3.21. Fig. 8(a) shows the simple Randles circuit that is used to fit the impedance data in the absence of inhibitor. It consists of solution resistance (R_s), constant phase element (CPE) in parallel with a charge transfer resistance (R_{ct}). An equivalent circuit of five elements is used to analyse the impedance data in the presence of HMBHC as shown in Fig. 8 (b). It consists of solution resistance R_s , charge transfer resistance R_{ct} , film resistance R_f and constant phase elements CPE_1 and CPE_2 . The CPE was introduced in the circuit instead of pure double layer capacitor (C_{dl}) to give more accurate fit. The impedance of CPE can be given by the expression (10).²²

$$Z_{CPE} = \frac{1}{Y_0(j\omega)^n} \quad (10)$$

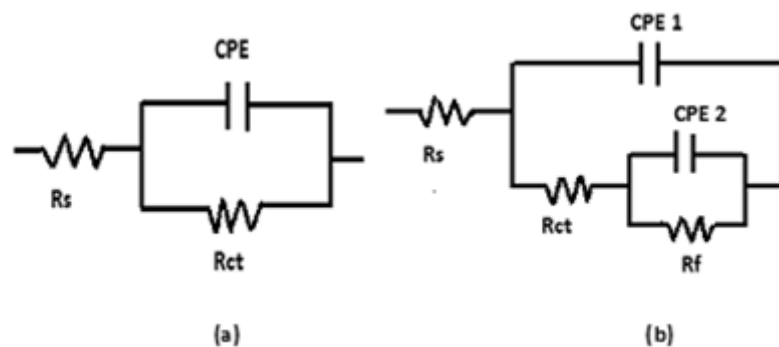


Fig. 8 – Equivalent circuits used to fit experimental EIS data for the corrosion of mild steel in 1 M HCl medium in the (a) absence of HMBHC and (b) presence of HMBHC.

Table 4

EIS results for mild steel in 1 M HCl in the absence and presence of different concentrations of HMBHC

Temp. (°C)	Conc. of inhibitor (mM)	R_{ct} ($\Omega \text{ cm}^{-2}$)	C_{dl} (μFcm^{-2})	IE (%)
30	0	15.7	1785	-
	0.1	78.6	134.02	80.0
	0.2	85.5	100.02	81.6
	0.4	134.7	59.16	88.3
	0.6	150.6	50.48	89.5
	0.8	170.5	39.31	90.6
40	0	9.63	3761	-
	0.1	50.5	309.43	80.9
	0.2	52.5	285.06	81.7
	0.4	66.8	202.18	85.6
	0.6	83.3	133.02	88.4
	0.8	95.2	108.61	89.8

Where Y_0 is the proportionality coefficient, w is the angular frequency, j is the imaginary number and n is the exponent related to the phase shift. If the value of $n=1$, the CPE behaves like an ideal double layer capacitance (C_{dl}). The correction in the capacitance to its real value was calculated using the relation (11).²³

$$C_{dl} = Y_0 (W_{max})^{n-1} \quad (11)$$

It is observed from the Table 4 that the values of C_{dl} decreases with increase in inhibitor concentrations at all studied temperatures. The decrease in C_{dl} is due to the increase in electrical double layer at the metal solution interface and by the gradual replacement of water molecules owing to the adsorption of organic molecules on the metal surface.²⁴

Table 4 (continued)

50	0	5.7	12936	-
	0.1	30.4	683.81	81.2
	0.2	32.1	616.76	82.1
	0.4	41.0	398.42	86.1
	0.6	46.5	320.33	87.7
	0.8	56.0	256.86	89.8
60	0	1.9	55870	-
	0.1	15.1	2642.9	87.3
	0.2	22.3	1166.19	91.4
	0.4	25.3	993.51	92.4
	0.6	30.5	736.57	93.7
	0.8	35.2	629.69	94.6

The charge transfer resistance R_{ct} is a measure of resistance against electron transfer across the surface and is inversely proportional to corrosion rate. Further, the R_{ct} values increase with increase in inhibitor concentration, which indicates that the corrosion process is mainly controlled by charge transfer process.²⁵ The R_{ct} is used to calculate the percentage inhibition (% IE).

$$\%IE = \frac{R_{ct} - R_{ct}^0}{R_{ct}} \times 100 \quad (12)$$

Where, R_{ct} and R_{ct}^0 indicate the charge transfer resistance in presence and absence of HMBHC.

Inhibition mechanism

Corrosion inhibitive action of HMBHC on mild steel in 1M hydrochloric acid solution can be explained on the basis adsorption phenomenon. The presence of free electron pairs in the sulphur, oxygen and the nitrogen atoms, π -electrons on the aromatic rings, imine group and molecular size of

HMBHC might have played a vital role in the adsorption of the inhibitor and the formation of coordinate bond with metal. The adsorbed HMBHC form a protective film on the metal surface, which acts as a barrier between metal and corrosive medium.²⁶

The mode of adsorption of HMBHC molecule on the mild steel surface is shown in Fig. 9(a) and 9(b). In a highly acidic solution, as in the present case, the HMBHC molecule can undergo protonation at its amino groups and can exist as a protonated positive species. Further, the metal surface is also gets positive charge in the presence of acidic medium. This would cause the negatively charged chloride ions to become adsorbed on the metal surface, making the metal surface negatively charged. The positively charged protonated HMBHC molecules can interact electrostatically with the negatively charged chloride adsorbed metal surface as shown in Fig. 9(a), resulting in physisorption particularly at lower temperature.²⁷

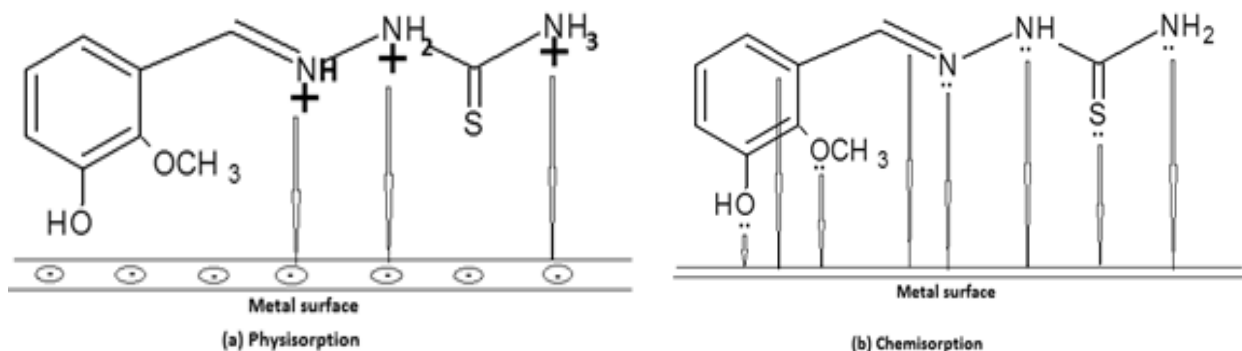


Fig. 9 – Skeletal representation of the mode of adsorption of HMBHC on mild steel surface.

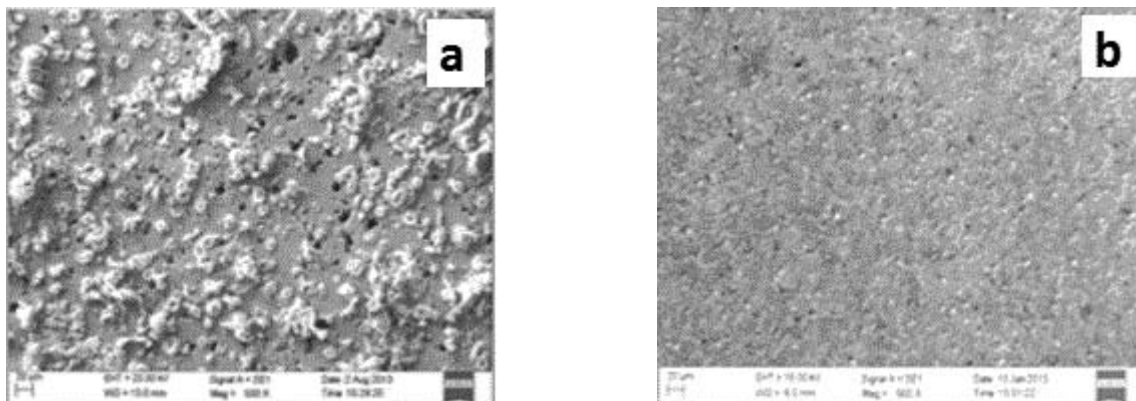


Fig. 10 – SEM images of the mild steel specimen surface (a) Exposed to 1 M HCl solution and (b) Exposed to 1 M HCl containing 0.8 mM of HMBHC.

The maximum inhibition efficiency attained at elevated temperature is due to the adsorption of HMBHC molecule on the surface of metal via chemisorption process. This is due to the displacement of the initially occupied water molecules from the surface of the metal leading to the sharing of electrons between the hetero atoms (O, S and N) and the metal. In addition, the horizontal orientation of the entire molecule with respect to the metal surface can also lead to donor-acceptor interaction of π -electrons of the aromatic ring with those vacant d orbitals of the metal surface resulting in chemisorption as shown in Fig. 9(b). The presence of imine group ($-\text{CH}=\text{N}-$) and electron donating groups (OH and OCH_3) in HMBHC makes it more effective and potential corrosion inhibitor for mild steel.²⁸

Scanning electron microscopy (SEM)

In order to differentiate between the surface morphology of the metal surface after its immersion in 1M HCl in the absence and presence of HMBHC, SEM investigations were carried out. Fig. 10 (a) shows the facets due to the corrosive action of 1 M HCl on the mild steel surface with cracks and rough surface. Smooth sample surface without any visible corrosion attack after immersion in 1 M HCl in the presence of HMBHC is shown in Fig. 10 (b). This indicates that HMBHC forms a uniform protective film on the specimen surface preventing it from undergoing corrosion.

CONCLUSIONS

Based on the results of investigation, the following conclusions are drawn:

HMBHC decreases both anodic and cathodic reactions, thereby acting as mixed type of inhibitor.

The inhibition efficiency increases with the increase in inhibitor concentration and increase in temperature.

HMBHC showed reasonably good inhibition efficiency (more than 90%) at optimum concentration (0.8 mM).

The adsorption of HMBHC on the metal surface follows Langmuir's adsorption isotherm.

The inhibition of corrosion takes place through the mixed adsorption of HMBHC with predominantly physisorption at the lower temperature and chemisorption at higher temperature.

There is a good correlation between Tafel polarization and EIS results.

REFERENCES

1. M. Mahdavian and S. Ashhari, *Electrochim. Acta*, **2010**, *55*, 1720-1724.
2. H. L. Wang, B. Liu and J. Xin, *Corros. Sci.*, **2004**, *46*, 2455-2466.
3. B. O. Renata, M. S. F. Elaine, P. P. S. Rodrigo, A. A. Anderson, U. K. Antoniana and L. Z. Carlos, *Eur. J. Med. Chem.*, **2008**, *43*, 1984-1988.
4. A. V. Shanbhag, T. V. Venkatesha, R. Prabhu, R. G. Kalkhambkar and G. M. Kulkarni *J. Appl. Electrochem.*, **2008**, *38*, 279-287.
5. G. E. Badr, *Corros. Sci.*, **2009**, *51*, 2529-2536.
6. M. G. Fontana. "Corrosion Engineering", McGraw-Hill, Singapore, 3rd edition, 1987
7. M. Shahin, S. Bilgic and H. Yilmaz, *Appl. Surf. Sci.*, **2002**, *195*, 1-7.
8. W. Li, Q. He, S. Zhang, C. Pei and B. Hou, *J. Appl. Electrochem.*, **2008**, *38*, 289-295.
9. G. Avci, *Colloids Surf A*, **2008**, *317*, 730-736.
10. M. Lebrini, F. Bentiss, H. Vezin and M. Lagrenée, *Corros. Sci.*, **2006**, *48*, 1279-1291.

11. H. L. Wang, H. B. Fan and J. S. Zheng, *Corros. Sci.*, **2004**, *46*, 2455-2454.
12. J. Yahalom, *Corros. Sci.*, *12* (1972) 867-875.
13. M. A. Ameer, E. Khamis and G. Al-Senani, *J. Appl. Electrochem.*, **2002**, *32*, 149-156.
14. A. S. Fouda, F. E. Heikal and M. S. Radwan, *J. Appl. Electrochem.*, **2009**, *39*, 391-342.
15. A. M. Fekry and M. A. Ameer, *Int. J. Hydration Energy*, **2010**, *35*, 7641-7651.
16. O. Olivares, N. V. Likhanova, B. Gomez, J. Navarrete, M. E. Llanos-Serrano, E. Arce and J. M. Hallen, *Appl. Surf. Sci.*, **2006**, *252*, 2894-2909.
17. I. Ahamad, R. Prasad and M. A. Quraishi, *Corros. Sci.*, *2010*, *52*, 933-942.
18. M. Hosseini, S. F. L. Mertens and M. Arshadi, *Corros. Sci.*, **2003**, *32*, 1473-1489.
19. E. E. N. Oguzie, V. O. Joku, C. K. Enenebeaku, C. O. Akalezi and C. Obi, *Corros. Sci.*, **2008**, *50*, 3480-3486.
20. G. R. Fuchs, *Colloids Surf. A.*, **2006**, *280*, 130-139.
21. K. Jutner, *Electrochim. Acta*, **1990**, *35*, 1501-1508.
22. E. Barsoukov and J. R. Macdonald, "Impedance Spectroscopy, Theory, Experiment and Applications", John Wiley & Sons, Hoboken, New Jersey, 2nd edn. 2005, p. 13-15.
23. C. H. Hsu and F. Mansfeld, *Corrosion*, **2001**, *57*, 747-748.
24. F. Bentiss, M. Traisnel and M. Lagrenee, *Corros. Sci.*, **2000**, *42*, 127-146.
25. S. Issaadi, T. Douadi, A. Zouaoui, S. Chafaa, M. A. Khan and G. Bouet, *Corros.Sci.*, **2011**, *53*, 1484-1488.
26. J. O. M. Bockris, M. A. Devanathan, and K. Mülle, *Proceedings of the Royal Society A*, **1963**, *274*, 55-79.
27. M. A. Elayyachy, A. E. I. Idrissi, B. Hammouti, *Corros. Sci.*, **2006**, *48*, 2470-2479.
28. K. C. Emregul, E. Duzgun and O. Atakol, *Corros. Sci.*, **2006**, *48*, 3243-3260.

